We are IntechOpen,
the world's leading publisher of
Open Access books
Built by scientists, for scientists

4,800
Open access books available

122,000
International authors and editors

135M
Downloads

154
Countries delivered to

Our authors are among the

TOP 1%
most cited scientists

12.2%
Contributors from top 500 universities

CLARIVATE ANALYTICS
BOOK CITATION INDEX
INDEXED

WEB OF SCIENCE™

Selection of our books indexed in the Book Citation Index
in Web of Science™ Core Collection (BKCI)

Interested in publishing with us?
Contact book.department@intechopen.com

Numbers displayed above are based on latest data collected.
For more information visit www.intechopen.com

Empires: The Nonlocal Properties of Quasicrystals

*Fang Fang, Sinziana Paduroiu, Dugan Hammock
and Klee Irwin*

Abstract

In quasicrystals, any given local patch—called an emperor—forces at all distances the existence of accompanying tiles—called the empire—revealing thus their inherent nonlocality. In this chapter, we review and compare the methods currently used for generating the empires, with a focus on the cut-and-project method, which can be generalized to calculate empires for any quasicrystals that are projections of cubic lattices. Projections of non-cubic lattices are more restrictive and some modifications to the cut-and-project method must be made in order to correctly compute the tilings and their empires. Interactions between empires have been modeled in a game-of-life approach governed by nonlocal rules and will be discussed in 2D and 3D quasicrystals. These nonlocal properties and the consequent dynamical evolution have many applications in quasicrystals research, and we will explore the connections with current material science experimental research.

Keywords: quasicrystals, empire, nonlocality, Penrose tiling, cut-and-project

1. Introduction

Quasicrystals are objects with aperiodic order and no translational symmetry. These "peculiar" objects, deemed in and out of existence by theoretical considerations, have been discovered in 1982 by Shechtman [1], in agreement with previous predictions [2, 3]. Shechtman's discovery was honored with the award of the Nobel Prize in Chemistry in 2011. Believed to be rare in nature initially, up to this date there have been found roughly one hundred quasicrystal phases that exhibit diffraction patterns showing quasiperiodic structures in metallic systems [4, 5]. Quasicrystals were first constructed as aperiodic tilings defined by an initial set of prototiles and their matching rules; constructing these tilings meant aggregating tiles onto an initial patch so as to fill space, ideally without gaps or defects. Likewise, quasicrystals in physical materials are formed by atoms accumulating to one another according to the geometry of their chemical bonding. Curiously, the localized growth patterns would give rise to structures which exhibit long-range and nonlocal order, and mathematical constructions were later discovered for creating geometrically perfect, infinite quasi-periodic tilings of space. In material science, new electron crystallography methods and techniques have been developed to study the structure and geometrical patterns of quasicrystal approximants [6–8], revealing unique atom configurations of complicated quasicrystal approximant structures [7, 8].

Complex and varied in their structure, quasicrystals translate their intrinsic nonlocal properties into nonlocal dynamic patterns [9]. The empire problem is an investigation into the nonlocal patterns that are imposed within a quasicrystal by a finite patch, where just a few tiles can have a global influence in the tiling so as to force an infinite arrangement of other tiles throughout the quasicrystal [10]. Initial research into calculating empires—a term originally coined by Conway [11]— focused on the various manifestations of the Penrose tiling [12] such as the deco- rated kites-and-darts, where Ammann bars would indicate the forced tiles [10], and the multi-grid method, where algebraic constraints can be employed [13]. More recently, the cut-and-project technique [14, 15]—where the geometry of convex polytopes comes into play—has been implemented into a most efficient method of computing empires [16]. The cut-and-project method offers the most generality and has been used to calculate empires for the Penrose tiling and other quasicrystals that are projections of cubic lattices $\mathbb{Z}^n$ [16, 17]. Quasicrystals that are projections of non-cubic lattices (e.g., the Elser-Sloane tiling as a projection of the E_8 lattice to $\mathbb{E}^4$) are more restrictive and some modifications to the cut-and-project method have been made in order to correctly compute the tilings and their empires [18]. The cut- and-project formalism can also be altered to calculate the space of all tilings that are allowed by a given patch, wherein the set of forced tiles of the patch's empire is precisely the mutual intersection of all tilings which contain that patch [15].

The interest in the nonlocal nature of empires has led to further explorations into how multiple empires can interact within a given quasicrystal, where separate patches can impose geometric restrictions on each other no matter how far apart they may be located within the tiling. These interactions can be used to define rules (similar to cellular automata) to see what dynamics emerge from a game-of-life style evolution of the quasicrystal and for the first time such a simulation with nonlocal rules has been performed [17].

The empires can be used to recover information from the higher dimensional lattice from which the quasicrystal was projected, filtering out any defects in the quasicrystal and therefore providing an error self-correction tool for quasicrystal growth [16]. In terms of quasicrystal dynamics, the empires provide us with the opportunity of developing algorithms to study the behavior and interactions of quasicrystalline patches based on nonlocal rules—a very rich area of exploration.

In this chapter we review the nonlocal properties of quasicrystals and the studies done to generate and analyze the empires and we discuss some of the findings and their possible implications.

2. Empires in quasicrystals

Empires represent thus all the tiles forced into existence at all distances by a quasicrystal patch. When it comes to analyzing the forced tile distribution in a quasicrystal, we differentiate between the local and nonlocal configurations. The tiles surrounding the vertex, that is the tiles that share one vertex, form the vertex patch. The local empire is the union of forced tiles that are in the immediate vicinity of an emperor, be it a vertex or a patch, where there are no "free" tiles in between the emperor and the forced tiles. The forced tiles that are at a distance from the emperor form the nonlocal part of the empire.

2.1 Methods for generating empires

Several methods for generating the empires in quasicrystals have been discussed in [16]. The Fibonacci-Grid method employs the Penrose tiling decoration using Amman bars that form a grid of five sets of parallel lines [10, 19]. The grid

constructed with the Amman bars is, in fact, a Fibonacci grid [20]. When Amman lines intersect in a certain configuration, a tile or a set of tiles are forced. The multigrid method [13] describes a tiling that can be constructed using a dual of a pentagrid, a superposition of five distinct families of hyperplanes in the case of Penrose tiling. It can be used for generating empires in cases where the dual grid for the quasicrystal has a simple representation, but it is not effective when the quasi-crystal has a defect, as its dual is no longer a perfect multigrid.

The most efficient method of generating empires in quasicrystals is the cut-and-project method. While the cut-and-project method and the multigrid one are mathematically equivalent in their use of generating empires, the cut-and-project method provides us with the possibility of recovering the initial mother lattice, even for defected quasicrystals [16]. The method has also been applied to projections of non-cubic lattices, making it of general use [18].

When we project from a lattice $\Lambda \subset \mathbb{E}^N$ $\pi_\parallel, \pi_\perp$ onto orthogonal subspaces $\mathbb{E}_\parallel, \mathbb{E}_\perp$, the *cut-window*, which is a convex volume $\mathcal{W}$ in the perpendicular space $\mathbb{E}_\perp$, determines the points selected to have their projections included in the tiling of the subspace $\mathbb{E}_\parallel$, acting thus as an acceptance domain for the tiling. Once the tiling is generated, all the tiles in a given local patch can be traced back to the mother lattice, giving a restriction on the cut-window. The *possibility-space-window* represents the union of all cut-windows that satisfy the restriction—all the tiles in the possibility-space-window *can* legally coexist with the chosen patch. The *empire-window* represents the intersection of all the possible cut-windows—all the tiles inside the empire-window *must* coexist with the initial patch. This in turn acts as the cut-window for the forced tiles, the patch's empire.[1]

For cubic lattices ($\Lambda = \mathbb{Z}^N$) the cut-window is sufficient for determining the tiles which fill the tiling space $\mathbb{E}_\perp$, but it needs to be sub-divided into regions acting as acceptance domains for individual tiles, when projecting non-cubic lattices.

To review some of the results of applying the cut-and-project method to the calculation of empires, we will give several examples in 2D and 3D cases.

2.2 Empires in 2D

For the 2D case, we will consider the Penrose tiling, a non-periodic tiling, a quasicrystal configuration that can be generated using an aperiodic set of prototiles. The 2D Penrose tiling, when projected from the cubic lattice $\mathbb{Z}^5$, has eight vertex types: D, J, K, Q, S, S3, S4 and S5 [21, 22]. In **Figure 1**, we show the empires for three of the vertex types that do not present five-fold symmetry (D, K, S4) computed with the cut-and-project method along with their possibility space [16]. The S4 vertex has the densest empire, while the D vertex has no forced tiles. The density of the empire depends on the size of the empire window, individual for each vetex type. In **Figure 2**, we show the empires and the possibility space of the five-fold symmetry vertex types, S5 (the star) and S (the sun) [16]. The empires of all 8 vertex types are displayed in [16].

2.3 Empires in 3D

The cut-and-project method described above can be used also for computing the empires of a given patch in 3D, e.g., an Amman tiling defined by a projection of $\mathbb{Z}^6$ to $\mathbb{E}^3$ [18]. In **Figure 3**, we show three orientations of the empires of two of the vertex types for this projection and we can see they differ in structure, as well as in density. Two other vertex types together with their empires are shown in [18].

---

[1] For a detailed description of this method and a comparison with the other methods, please refer to [16].
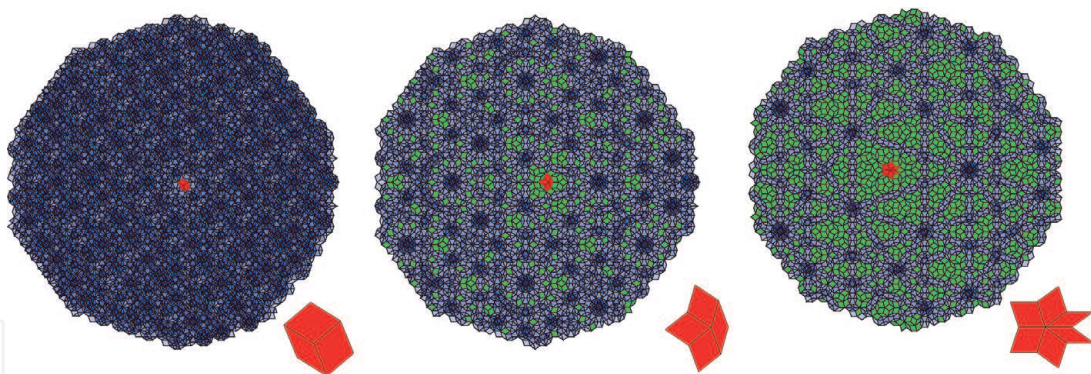
Figure 1.
Empire calculation of the vertex types D (left), K (middle) and S4 (right). The red tiles represent the vertex patch and the green tiles represent the empire. The enlarged vertex patch is shown in the right corner for each case. The pictures for all vertex types have been published in [16], Figures 13 and 14.
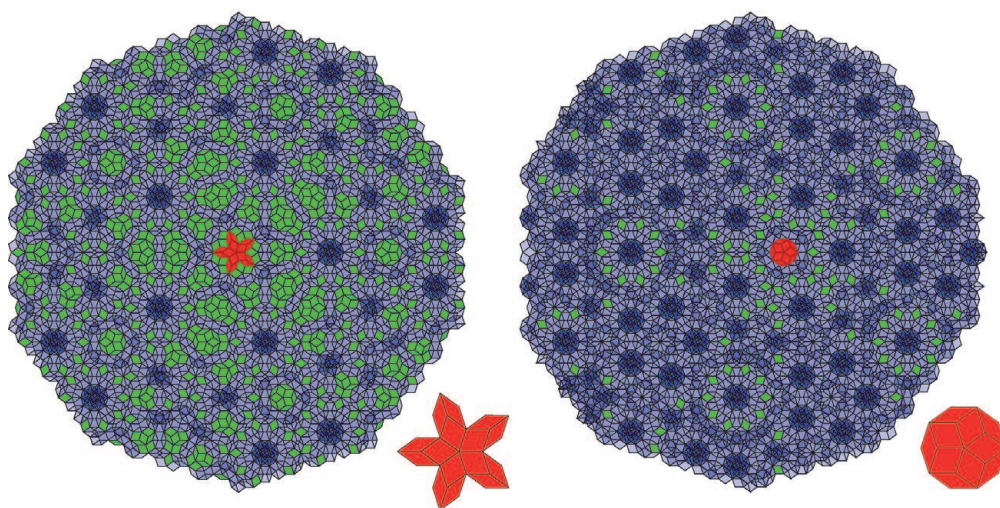

Figure 2.
Empire calculation for the vertex types S5 (left) and S (right). The red tiles represent the vertex patch and the green tiles represent the empire. The enlarged vertex patch is shown in the right corner for each case. The pictures for all vertex types have been published in [16], Figures 13 and 14.

Furthermore, the method can be used also for non-cubic lattices, but it requires some adjustment, as the proper selection of the tiles becomes more complex. It has been shown [18] that the cut-window must be sub-divided into regions, which act as acceptance domains for individual tiles and can be used to compute both the relative frequencies of the vertex's configuration and the empire of a given tile configuration. The authors have used the method to compute the frequencies and sectors for an icosahedral projection of the D_6 lattice to $\mathbb{E}^3$, which has 36 vertex configurations [23] and have compared their findings with previous results [23–25].

3. Quasicrystal dynamics

The inherent nonlocal properties of quasicrystals allow us to study different dynamical models of self-interaction and interactions between different vertex configurations in quasicrystals, using the empires. Several game-of-life [21] algorithms have been previously studied on Penrose tiling, but they have either considered a periodic grid [26] or they have considered only local rules [27, 28]. Recently, for the first time, a game-of-life scenario has been simulated using nonlocal rules on a two-dimensional qusicrystal, the Penrose tiling, in [17]. In this simulation, for the K vertex type, the emperor and its local patch are treated as a quasiparticle, a glider.
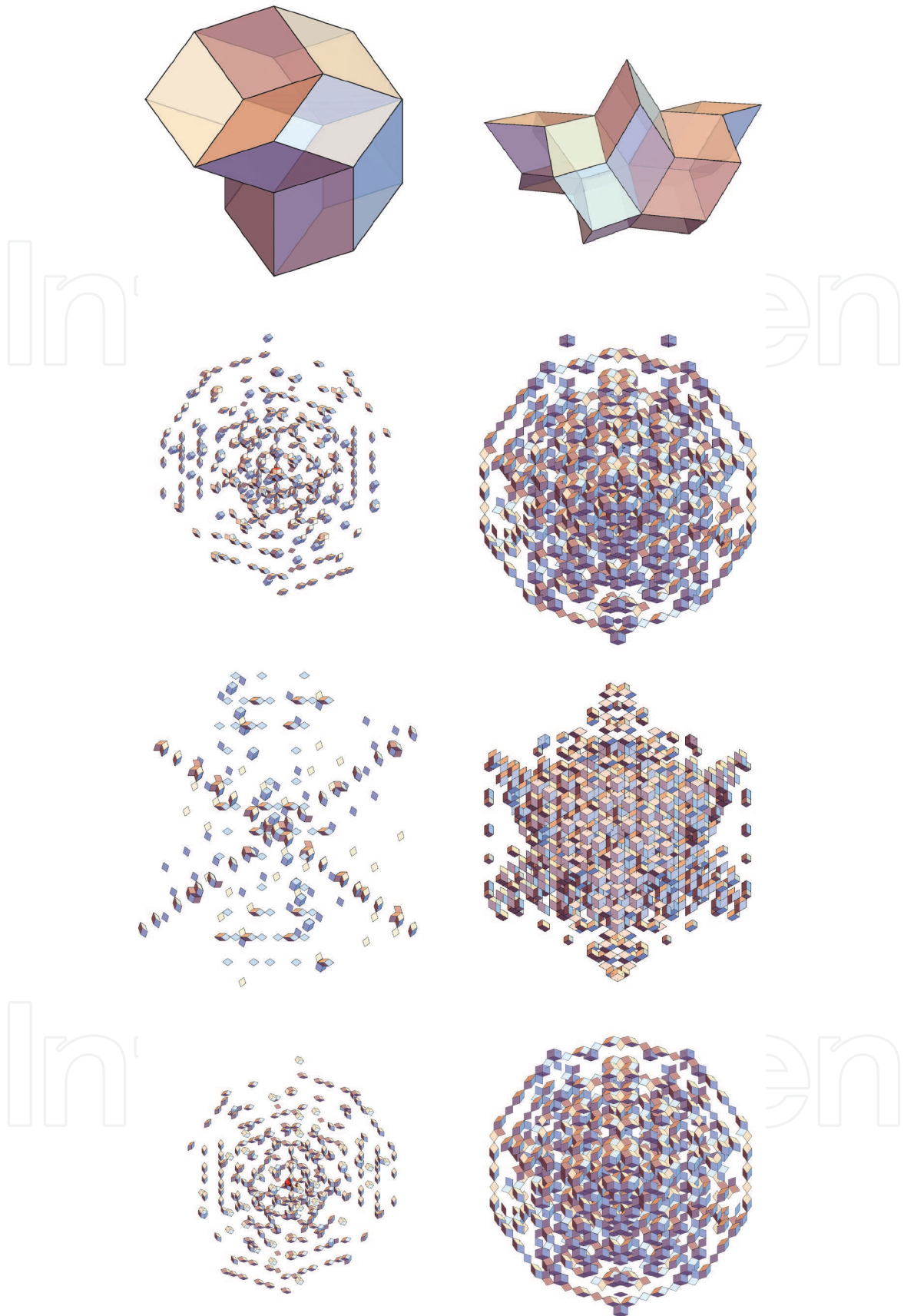
Figure 3.
Vertex configurations and their empires for the Ammann tiling as projected from $\mathbb{Z}^6$ to $\mathbb{E}^3$. The tiles of this quasicrystal are all rhombohedrons, and the vertex configurations are analogous to those of the Penrose tiling. The empires are shown in three orientations below the vertex configurations. Other two vertex configurations and their empires have been shown in [18] Figure 9.

The empire acts as a field and the interaction between two quasiparticles is modeled as the interaction between empires.

Several rules have been employed to describe both the self-interaction and the two-particle interactions. Firstly, the neighbors where the vertex patch is allowed to move are constrained by the higher dimensional projection, being the closest neighbors of the same vertex type in the perpendicular space. This approach differs from previous studies that consider the nearest neighbors situated in the local 2D representation [27, 28]. In **Figure 4**, one can see the K vertex type and 2D representation of the nearest neighbors in the perpendicular space that we have considered [17]. The distribution of the neighbors is interesting, as it surrounds an S vertex patch (sun) on one side and an S5 vertex patch (star) on the other side. We will expand on this configuration in the next section.

Secondly, the vertex never stays in the same position for two consecutive frames, being thus forced to move to one of the allowed neighbors in its immediate vicinity. Depending on the intrinsic configuration of the vertex patch, some vertices allow more freedom of movement than others. For example, a vertex with a five-fold symmetry will tend to perform a "circular" motion around its axis of symmetry, a rotation, while a vertex without the five-fold symmetry, like the K vertex, will have the possibility to propagate forward, the translational movement being a sequence of rotations around different centers.

Moreover, the particle moves following the "least change" rule, which states that the particle should move to the position (or one of the positions) where the result of that movement implies that the number of tiles changed in the empire is minimum. In other words, the particle will follow the path that requires the least number of changes in the tiles in the empire, while not being allowed to stay in the same position for two consecutive frames. When there is more than one choice that obeys the aforementioned rules, a random-hinge variable is introduced such that the particle will chose one of the favored positions. Due to the syntactical freedom provided by this choice, the path of a particle, unless constrained otherwise, is impossible to predict with 100% accuracy.

For the case of two-particle interactions, one more arbitrary constraint is introduced, where the local patches of the two particles are not allowed to overlap. A detailed discussion of the algorithm and the simulation setup can be found in [17].[2]
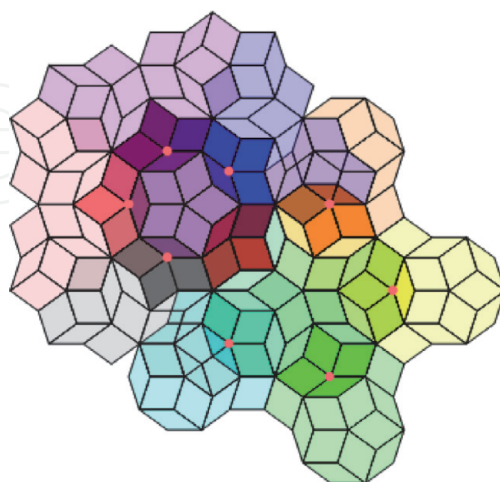

Figure 4.
The K vertex type surrounded by the eight possible neighbors. The orange dots represent the position of the K vertices that surround the star and sun vertex patches.

---

[2] Movies from the simulations can be watched on https://www.youtube.com/playlist?list=PL-kqKe jCypNT990P0h2CFhrRCpaH9e858.

Besides the initial conditions, meaning the vertex type configuration and the initial position of the particles in the two-particle interaction case, the movement of the particles is influenced solely by their empires and their possibility space. When the empire changes, the possibility space changes as well, constraining the next move due to the new spatial configuration. The empire and the possibility space create a feedback loop of influence, which for an infinite quasicrystal propagates instantly at infinite distances.

One of the most interesting findings is that in the case of the two-particle interactions, the particles get locked in an oscillation type movement when they are in proximity. If we consider an analogy between the "least change" principle—the number of tiles that change between two steps is minimum—and a minimum energy principle, the system tends to reach a minimum energy state in oscillation. This is similar with the time crystal scenarios [29–32] where a system disturbed by a periodic signal reaches a quasistable state in which it oscillates at a period different from the period of the external kick. In this case, a quasiparticle will draw stability from its empire interaction with other quasiparticles' empires—a nonlocal induced stability.

4. Empires and higher dimensional representations

Quasicrystals projected from a higher dimensional lattice, $\mathbb{Z}^5$ for example, show several properties dictated from the representation in the high dimension, like the symmetry and the vertex and empire distribution. As discussed previously, for the K vertex type, the nearest neighbors considered in the game-of-life scenario are also dictated by the higher dimensional lattice from which the tiling is projected, being the closest neighbors in the perpendicular space [17].

In **Figure 4**, we have shown the K vertex type with its eight neighbors that surround a sun and a star configuration. **Figure 5** shows the sun vertex patch surrounded by the five orientations of the K vertex type. This is a more complex structure that has five-fold symmetry. When choosing only the sun configurations that are bordered by the K-type vertices, we observe that these configurations come from two different regions in the perpendicular space. In **Figure 6**, we show the 2D distribution of the K-type vertices, plotted in two different colors, corresponding to the two distinct regions in the perpendicular space from which the vertices are projected. The vertices form interesting patterns on the Penrose tiling. **Figure 7**
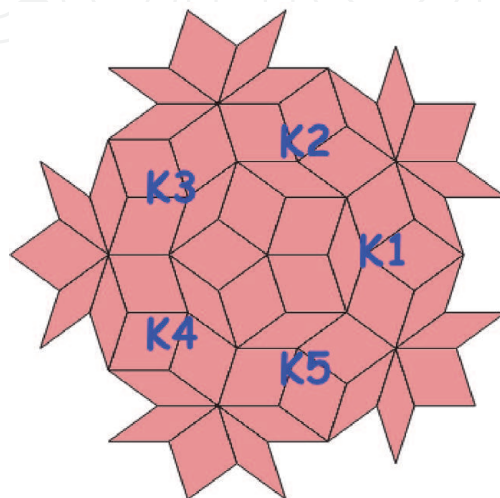

Figure 5.
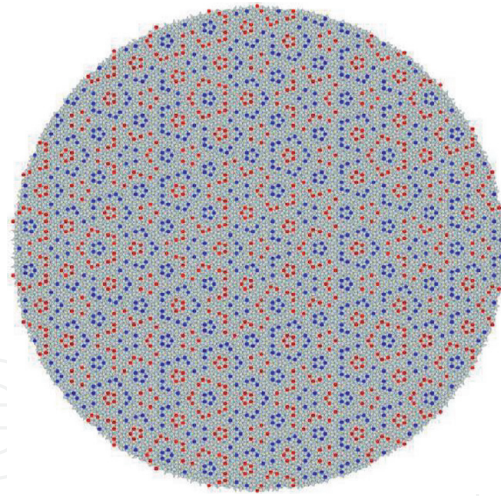*The sun configuration surrounded by the five different orientations of the K-type vertex patch.*

Figure 6.
The K-type vertex distribution plotted in two different colors, one for each of the distinct regions in the perpendicular space from where these configurations are projected.
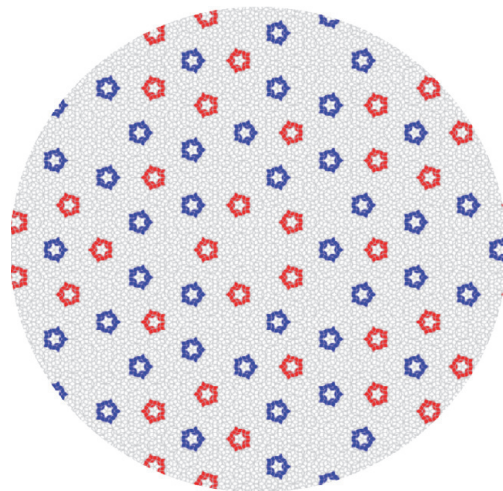

Figure 7.
Sun configurations surrounded by the five orientations of the K-type vertex plotted in two different colors corresponding to the two distinct regions in the perpendicular space from where these configurations are projected.
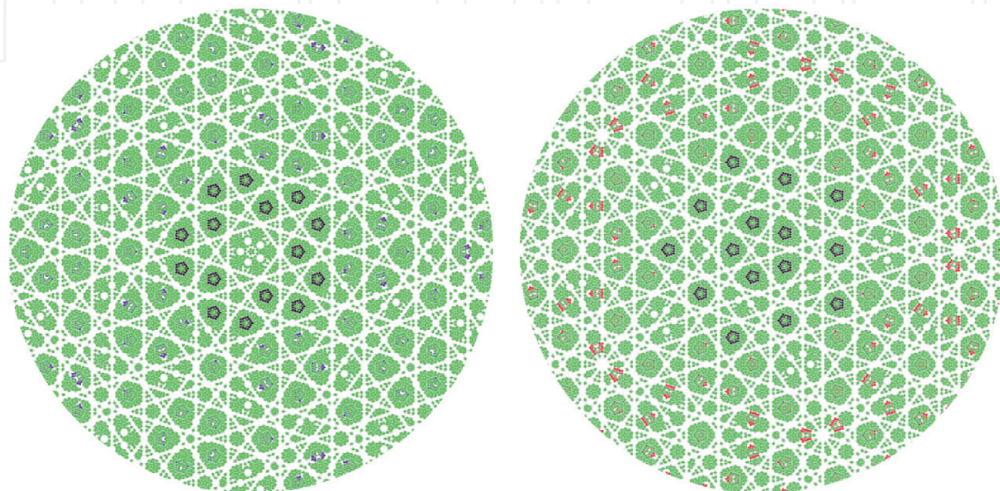

Figure 8.
Sun configurations surrounded by K vertex types from different regions in the perpendicular space displayed side-by-side. The black tiles represent the vertices with their empires turned on. The empires are colored in green.

shows a zoom-in region where only the sun configurations surrounded by K-type vertices are plotted also in different colors.

We have performed several studies of the empires of the K-type vertices that surround sun configurations. When analyzing just the K-sun configurations projected from the same region in the perpendicular space we are looking at the empire distributions, considering the empires from the K vertices. We consider one sun configuration to be completed, when all the K vertices surrounding it have their empires turned on. One of the interesting findings is that regardless of the number of completed suns—K vertex empires turned on—no other K vertex type surrounding a sun is covered by these empires. The K vertex patch tiles closest to the center—the sun—remain uncovered by the empires from the other suns. This is valid also for the case in which the sun configurations are projected from the other region in the perpendicular space. Provided these configurations are from the same region in the perpendicular space, there are some tiles in the K vertices that are not covered by empires coming from different suns—a "selective" nonlocality constrained by the higher dimensional representation. In **Figure 8**, we show the K-sun configurations side-by-side from both distinct regions in the perpendicular space.

5. Conclusions

In this chapter we have reviewed several properties of quasicrystals, their nonlocal empires, and the methods used to generate the quasicrystal configurations and the empires of their vertices. We have studied quasicrystals projected from higher dimensions, $\mathbb{Z}^5$ to 2D (the Penrose tiling), $\mathbb{Z}^6$ to $\mathbb{E}^3$ and $\mathbb{D}^6$ to $\mathbb{E}^3$ for the 3D case. For several vertex configurations, we have analyzed their empires—the nonlocal distribution of their forced tiles—in relation to the higher dimension representation. These nonlocal properties allow us to study the quasicrystal dynamics in a novel way, a nonlocal game-of-life approach, in which the empires and the possibility space dictate the movement and trajectory of the chosen quasiparticle configurations. Case studies of two-particle interactions based on nonlocal rules, while not exhaustive, are showing important similarities with other experimental physics discoveries, like time crystals. The research into the inherent nonlocality of quasicrystals proves very rich in describing the various quasicrystal configurations and their correlation with high dimensional representations. These studies open up a new, but very promising avenue of research that can bridge together different fields, like physics in high dimensions, gauge and group theory, phason dynamics and advanced material science.

Acknowledgements

Author details

Fang Fang*[†], Sinziana Paduroiu[†], Dugan Hammock and Klee Irwin
Quantum Gravity Research, Los Angeles, CA, USA

*Address all correspondence to: fang@quantumgravityresearch.org

[†] These authors contributed equally.

IntechOpen

References

[1] Shechtman D, Blech I, Gratias D, Cahn JW. Metallic phase with long-range orientational order and no translational symmetry. Physical Review Letters. 1984;**53**:1951. DOI: 10.1103/PhysRevLett.53.1951

[2] Kleinert H, Maki K. Lattice textures in cholesteric liquid crystals. Fortschritte der Physik. 1981;**29**:219259. DOI: 10.1002/prop.19810290503

[3] Levine D, Steinhardt PJ. Quasicrystals: A new class of ordered structures. Physical Review Letters. 1984;**53**:2477. DOI: 10.1103/PhysRevLett.53.2477

[4] Murr LE. Aperiodic crystal structures: Quasicrystals. Handbook of Materials Structures, Properties, Processing and Performance. Switzerland: Springer; 2014. pp. 1-9. DOI: 10.1007/978-3-319-01815-7

[5] Steurer W. Twenty years of structure research on quasicrystals. Part I. Pentagonal, octagonal, decagonal and dodecagonal quasicrystals. Zeitschrift für Kristallographie – Crystalline Materials. 2004;219:391-446. DOI: 10.1524/zkri.219.7.391.35643

[6] Hovmoller S, Hovmoller ZL, Zou X, Grushko B. Structures of pseudo-decagonal approximants in Al-Co-Ni. Philosophical Transactions of the Royal Society of London, Series A. 2012;**370**: 2949. DOI: 10.1098/rsta.2011.0310

[7] Singh D, Yun Y, Wan W, Grushko B, Zou X, Hovmoller S. A complex pseudo-decagonal quasicrystalapproximant, $Al_{37}(Co, Ni)_{15.5}$, solved by rotation electron diffraction. Journal of Applied Crystallography. 2014;**47**:215. DOI: 10.1107/S1600576713029294

[8] Singh D, Yun Y, Wan W, Grushko B, Zou X, Hovmoller S. Structure determination of a pseudo-decagonal quasicrystal approximant by the strong-reflections approach and rotation electron diffraction. Journal of Applied Crystallography. 2016;**49**:433-441. DOI: 10.1107/S1600576716000042

[9] Nagao K, Inuzuka T, Nishimoto K, Edagawa K. Experimental observation of quasicrystal growth. Physical Review Letters. 2015;**115**:075501. DOI: 10.1103/PhysRevLett.115.075501

[10] Grunbaum B, Shephard GC. Tilings and Patterns. New York: W. H. Freeman and Company; 1987. DOI: 0.1002/crat.2170260812

[11] Conway JH. Triangle tessellations of the plane. American Mathematical Monthly. 1965;**72**:915

[12] Penrose R. The role of aesthetics in pure and applied mathematical research. Bulletin of the Institute of Mathematics and Its Applications. 1974;**10**:266

[13] Effinger L. The empire problem in penrose tilings [thesis]. Williamstown US: Williams College; 2006

[14] Socolar JES, Steinhardt PJ. Quasicrystals. II. Unit-cell configurations. Physical Review B. 1986;**34**:617. DOI: 10.1103/PhysRevB.34.617

[15] Senechal MJ. Quasicrystals and Geometry. Cambridge: Cambridge University Press; 1995. DOI: 10.1002/adma.19970091217

[16] Fang F, Hammock D, Irwin K. Methods for calculating empires in quasicrystals. MDPI Crystals. 2017;7: 304. DOI: 10.3390/cryst7100304

[17] Fang F, Paduroiu S, Hammock D, Irwin K. Non-local game of life in 2D quasicrystals. MDPI Crystals. 2018;**8**: 416. DOI: 10.3390/cryst8110416

[18] Hammock D, Fang F, Irwin K. Quasicrystal tilings in three dimensions

and their empires. MDPI Crystals. 2018;**8**:370. DOI: 10.3390/cryst8100370

[19] Minnick L. Generalized forcing in aperiodic tilings [thesis]. Williams College; 1998

[20] Fang F, Irwin K. An icosahedral quasicrystal and E8 derived quasicrystals. arXiv:1511.07786. 2015

[21] Gardner M. Mathematical games the fantastic combinations of John Conways new solitaire game of 'life'. Scientific American. 1970;**223**:120

[22] de Bruijn NG. Algebraic theory of Penroses non-periodic tilings. Proceedings of the Koninklijke Nederlandse Akademie van Wetenschappen. 1981;**84**:53. DOI: 0.1016/1385-7258(81)90017-2

[23] Papadopolos Z, Kramer P, Zeidler D. The F-type icosahedral phase: Tiling and vertex models. Journal of Non-Crystalline Solids. 1993;**153**:215. DOI: 10.1016/0022-3093(93)90345-X

[24] Kramer P, Papadopolos Z, Zeidler D. Symmetries of icosahedral quasicrystals. In: Gruber B, Biedenharn LC, Doebner HD, editors. Symmetries in Science V. Boston: Springer; 2011. p. 395. DOI:10.1007/978-1-4615-3696-3_19

[25] Kramer P. Modelling of Quasicrystals. Physica Scripta. 1993;**T49**:343. DOI: 10.1088/0031-8949/1993/T49A/060

[26] Bailey DA, Lindsey KA. Game of Life on Penrose Tilings. arXiv: 1708.09301. 2017

[27] Owens N, Stepney S. Investigations of Game of Life Cellular Automata Rules on Penrose Tilings: Lifetime and Ash Statistics. Automata-2008. Bristol: Luniver Press; 2008. p. 1

[28] Owens NDL, Stepney S. Investigations of game of life cellular automata rules on Penrose tilings: Lifetime, ash, and oscillator statistics. Journal of Cellular Automata. 2010;**5**: 207

[29] Wilczek F. Quantum time crystals. Physical Review Letters. 2012;**109**: 160401. DOI: 10.1103/PhysRevLett.109.160401

[30] Else DV, Nayak C. Classification of topological phases in periodically driven interacting systems. Physical Review B. 2016;**93**:201103. DOI: 10.1103/PhysRevB.93.201103

[31] Zhang J, Hess PW, Kyprianidis A, Becker P, Lee A, Smith J, et al. Observation of a discrete time crystal. Nature. 2017;**543**:217. DOI: 10.1038/nature21413

[32] Sacha K, Zakrzewski J. Time crystals: A review. Reports on Progress in Physics. 2018;**81**:016401. DOI: 10.1088/1361-6633/aa8b38